View metadata, citation and similar papers at core.ac.uk
brought to you by CORE
provided by University of Liverpool Repository

Uncertainties in the two-stage reception plate method for source characterisation and prediction of structure-borne sound power

B. M. Gibbs, G. Seiffert
Acoustics Research Unit, School of Architecture, University of Liverpool, UK

K. H. Lai
Noise, Vibration and Emissions, Boeing Commercial Airplanes, Seattle, Washington, USA

Summary

To obtain the transmitted structure-borne power from a vibrating machine into a supporting/connected structure, three quantities are required in some form: source activity (either the free velocity or the blocked force), source mobility and receiver mobility. The three quantities can be measured directly, or indirectly using a reception plate method. Whilst direct measurements can be precise, they require extensive data acquisition and processing. The reception plate method is simpler and less precise and therefore yields an engineering grade of accuracy. This paper reports on a collaborative investigation, towards developing an industrial standard for source characterization using the reception plate method. The method yields data as frequency band-averaged values and also as equivalent single values. These simplifications result in uncertainties when obtaining the source quantities and therefore in predictions of the structure-borne sound power in installed conditions. The causes of these uncertainties are considered.
PACS no. 43.40

1. Introduction

A structure-borne sound source characterization should lead to prediction of the transmitted power from a vibrating machine (the source) into a supporting structural element (the receiver). For this, three quantities are required prior to installation: source activity (either the free velocity or the blocked force); source mobility (or the inverse impedance); receiver mobility (or impedance) [1-3]. The three quantities can be measured precisely, for each contact and for up to six components of excitation (three translations and three rotations). However, the measurement and calculation effort is large and not all components of excitation need be considered. In building acoustics, the forces perpendicular to the receiver usually dominate the transmitted power [4-7] and this component only is considered. To further reduce the measurement effort, the three quantities are measured indirectly using the reception plate method (RPM). The obtained quantities are frequency band averaged values, e.g. in 1/3 octave bands; further the three quantities are expressed as equivalent single values. By equivalent is meant that for multi-contact sources, the source activity is the sum-square over the contacts and the source mobility is the average of the point mobility over the same contacts.

For the source quantities, the reception plate method requires the machine to be attached to a simple plate and operated under otherwise normal conditions [8]. The total power from the machine, through all contacts with the reception plate, equals the plate power, which is calculated from the plate parameters as [1]

$$P_{source} = P_{plate} = \omega \eta M \left\langle v^2 \right\rangle \qquad (1)$$

The mean-square plate velocity $\langle v^2 \rangle$ is recorded using accelerometers distributed over the plate surface. The loss factor η of the plate of mass *M* is obtained by the decay method [9]. Implicit is the assumption that the plate power is wholly determined by the plate bending energy and total loss factor [1]. Therefore, the source's contribution to the plate bending energy determines the source total power.

Alternatively, the plate can be calibrated with a shaker and in-line force transducer to give the ratio of a known input power P_{cal} to the mean square plate velocity $\langle v_{cal}{}^2 \rangle$ [10]. Replacing the instrumented shaker with the source under test then gives the required source power

$$P_{source} = \langle v_{source}{}^2 \rangle P_{cal} / \langle v_{cal}{}^2 \rangle \tag{2}$$

The total power transmitted from a machine, when attached to a plate structure, is calculated from the independent source and receiver quantities [11]

$$P = |v_f|^2 \frac{\mathrm{Re}(Y_R)}{|Y_S + Y_R|^2} \tag{3}$$

$|v_f|^2$ is the vector of the mean square free velocity over the contacts, Y_S is the complex source mobility and Y_R is the complex mobility of the receiver plate structure. Equation (3) is expressed in matrix form for multiple contacts.

The total power can be approximated by replacing the vector and matrix values with equivalent single quantities [6]

$$P \approx v_{feq}^2 \frac{\mathrm{Re}\,(Y_{Req})}{|Y_{Seq} + Y_{Req}|^2} \tag{4}$$

The equivalent single quantities can be obtained indirectly by attaching the operating source to a laboratory reception plate, i.e. a plate isolated from the laboratory floor. If the reception plate is thick, such that the plate mobility is much lower than the source mobility, then the source can be characterized by a single quantity, related to the sum square blocked force over the machine supports. Equation (4) reduces and the source power into a plate of known low mobility Y_{low} is approximately [12]

$$P_{low} \approx \frac{|v_{feq}|^2}{|Y_{Seq}|^2} \mathrm{Re}\,(Y_{low}) \approx F_{beq}^2 \mathrm{Re}\,(Y_{low}) \tag{5}$$

If the reception plate is thin, such that the plate mobility is much higher than source mobility, then the source can be characterized by a single quantity, related to the sum square free velocity over the

contacts [13]. Equation (4) reduces and the approximate source power into a plate of known high mobility Y_{high} is

$$P_{high} \approx v_{feq}^2 \ \mathrm{Re}(Y_{high}) / \left|Y_{high}\right|^2 = v_{feq}^2 \ \mathrm{Re}(1/Y_{high}) = v_{feq}^2 \ \mathrm{Re}(z_{high}) \tag{6}$$

Re-arranging the expressions in equations (5) and (6) gives approximations to the sum square blocked force over the *N* contacts and sum square free velocity over the *N* contacts, respectively

$$F_{beq}^2 \approx \sum_i^N F_{bi}^2 \ ; \ v_{feq}^2 \approx \sum_i^N v_{fi}^2 \tag{7}$$

The equivalent single source mobility is obtained from the single values in equation (7)

$$Y_{Seq} \approx \sqrt{v_{feq}^2 / F_{beq}^2} \tag{8}$$

The equivalent single source mobility approximates the average point mobility magnitude over the *N* contacts

$$Y_{Seq} \approx \sum_i^N \left|Y_i\right| \tag{9}$$

Any two of the RPM measured quantities, obtained from equations (5), (6) and (8), are used in combination with measured or calculated receiver mobility Y_{Req}, to calculate the structure-borne power in the installed situation, i.e. into any other plate-like supporting structure.

Equation (4) is further simplified to give

$$P_{installed} \approx v_{feq}^2 \frac{\mathrm{Re}\left(Y_{Req}\right)}{\left|Y_{Seq}\right|^2 + \left|Y_{Req}\right|^2} \tag{10}$$

On comparing equation (10) with equation (4), the complex relationship between source and receiver mobility, in the denominator of equation (4), is neglected in equation (10). As a result, errors are expected, particularly when the mobilities are of the same order [14]. Further, in assembling the equivalent single source mobility, the complex relationship between contact forces either has to be approximated [15] or neglected [6]. The simplifications and the resultant approximations give rise to uncertainties. In the following experimental implementation, the causes of the uncertainties are considered at each stage of the method.

2. Experimental implementation

Two sources were tested: a small air pump and a centrifugal fan. The pump was either rigidly attached or mounted on isolators. The sources were mounted, in turn, on two reception plates. The high mobility plate was of 1 mm perforated mild steel, in a 2m x 1m clamping frame, which was supported on elastic pads to reduce the effect of floor vibrations. The perforations increase the mobility and reduce acoustic feedback from sound pressures in the laboratory. The low mobility plate was of 20 mm aluminium (2.12m x 1.50m), resiliently supported on visco-elastic pads, to provide isolation and to introduce useful damping at low frequencies.

In Figure 1 are shown the point mobility magnitude of the two sources (as averages over four contacts) and of the two reception plates (as spatial averages over the plate surfaces; the low mobility plate value is shown as the real part). The high mobility reception plate is at least 5 dB greater than the source mobilities (based on the 10 log convention). This is less than the notional requirement of 10 dB level difference [4]. The mobility of the sources are more than 5 dB greater than that of the low mobility reception plate, except at 300 Hz, where the pump mobility is of the same order as that of the low mobility plate. The narrow-band values vary more with frequency and location, with matched conditions occurring in some narrow frequency bands. Increased power transmissions are expected, where the source and receiver mobilities are equal (particularly, when they are complex conjugates, see the denominator on equation (4)). However, the matching conditions are relatively rare and their effects tend to randomise out [14].

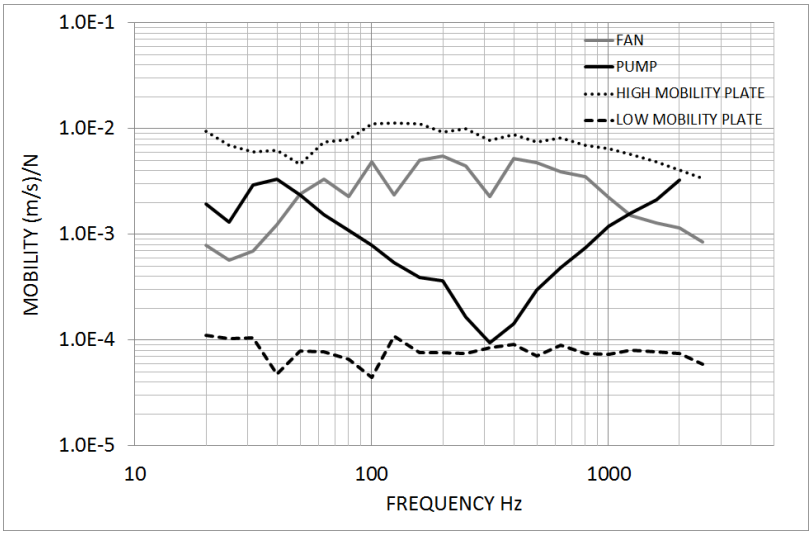

Figure 1. Average point mobility magnitude of the two sources and of the two reception plates.

As a test of the approximate approach, the two-stage estimates of the source quantities were used to calculate the power into two other plate structures: a clamped notched plate of 11mm aluminium and a 13 mm ribbed Perspex plate. The approximate powers then were compared with in situ measurements, obtained by power substitution, according to equation (2).

2.1. Free velocity by RPM

Figure 2, left, shows one of the tested sources, the air pump, when glued to the high mobility 1 mm clamped perforated steel plate. The source power was measured by power substitution, according to equation (2). The calibration power P_{cal} was obtained from the real part of the cross-spectrum $F_c^* v_c$. The calibration source was a shaker with in-line force transducer, shown in Figure 2 right, which registered the

contact force F_c . An accelerometer at or close to the contact point registered the contact velocity v_c . The average square velocity of the plate was obtained from seven remote accelerometer positions, for each of the shaker locations. The power calibration was undertaken with the test source attached, to allow for changes in the plate dynamics and losses, due to the attachment. Also required is the real part of plate impedance $\mathrm{Re}(z_{high})$, from equation (6).

Figure 2. Left: pump attached to the perforated plate with remote accelerometers; right: shaker with inline force transducer for power calibration.

The RPM free velocity squared v^2_{feq} is obtained by re-arranging equation (6). Figure 3, left shows the measured sum square free velocity of the pump and RPM estimate. For frequencies above 63 Hz, the agreement is generally within 10 dB. Below this frequency, the RPM gives an underestimate. This is partially the result of rigid body rocking motion of the compact pump, which gives reduced power into the reception plate. This is exemplified by including the measured complex sum square free velocity in Figure 3, left. However, the RPM estimate also depends in the power into the high mobility plate, which in turn depends on the modal behaviour of the plate.

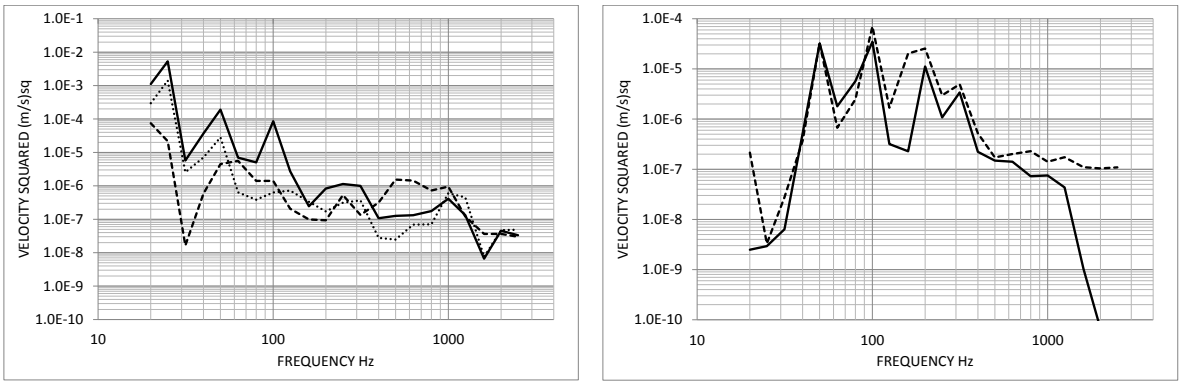

Figure 3. Left: pump sum square free velocity: measured (solid line); measured complex sum square (dotted); RPM estimate (dashed); right: for fan sum square free velocity.

Figure 3, right shows the measured sum square free velocity of the fan and RPM estimate. The tonal behaviour of the source is captured more clearly for the fan than for the pump, with agreement between measurement and RPM estimates within 3 dB at the peaks at 50 Hz, 100 Hz anf 200 Hz. The agreement is generally within 5 dB, except at 125 Hz and 160 Hz. The fan does not display rigid body behaviour; the contacts are at greater distances than for the pump and the contact forces can be assumed to behave independently. Over-estimates at high frequencies are generally the result of reduced signal-to-

noise in the reception plate measurements. However, the over-estimates occur when the levels are 20 to 30 dB below the maximum values. At these frequencies, the sources are not expected to be significant noise problems.

2.2. Blocked force by RPM

The RPM estimate of blocked force is obtained by attaching the test source to the low mobility 20mm aluminium plate and obtaining the power P_{low} from the source in operation. P_{low} was obtained from the power calibration in equation (2). Also required was the real part of the plate mobility $\mathrm{Re}\,(Y_{low})$. The heavy plate is not dynamical loaded by the test sources and the power calibration was conducted prior to their attachment.

Figure 4, left shows the sum square blocked force of the pump, from direct measurement of free velocity and source mobility, and by the RPM. The RPM estimate is within 5 dB of the measured value, above 63 Hz, with a negative discrepancy of 10 dB, below 63 Hz. The low frequency discrepancy again is likely due to rocking motion which gives reduced power into the plate. The RPM estimate for the fan (right) is within 5 dB of the measured value, except at 800 Hz.

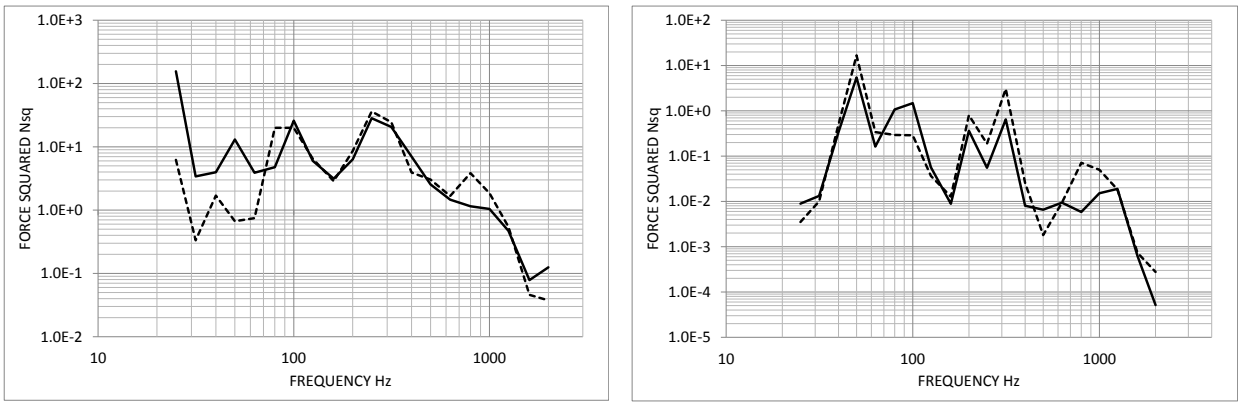

Figure 4. Left: pump sum square blocked force: from measured free velocity and source mobility (solid line); RPM estimate (dashed); right: fan sum square blocked force.

2.3. Source mobility by RPM

The RPM estimates of free velocity squared and blocked force squared can be used to estimate the source mobility, according to equation (8). Figure 5, left shows the measured magnitude of point mobility at the four contact points of the pump. Also shown are the average measured mobility and the RPM estimate. The measured point mobilities are within the range of 5 dB. The RPM estimate is within 5 dB of the average measured magnitude. The agreement is generally better than for the free velocity squared and blocked force squared at low frequencies and it is concluded that the low-frequency discrepancies partially cancel in the ratio in equation (8). Figure 5, right shows the measured average point mobility magnitude of the fan, with the RPM estimate. Also shown are the point mobility magnitudes at the four contacts. The measured point mobilities show a larger variation between contact pairs, than for the pump. The range is 15 dB at low frequencies.

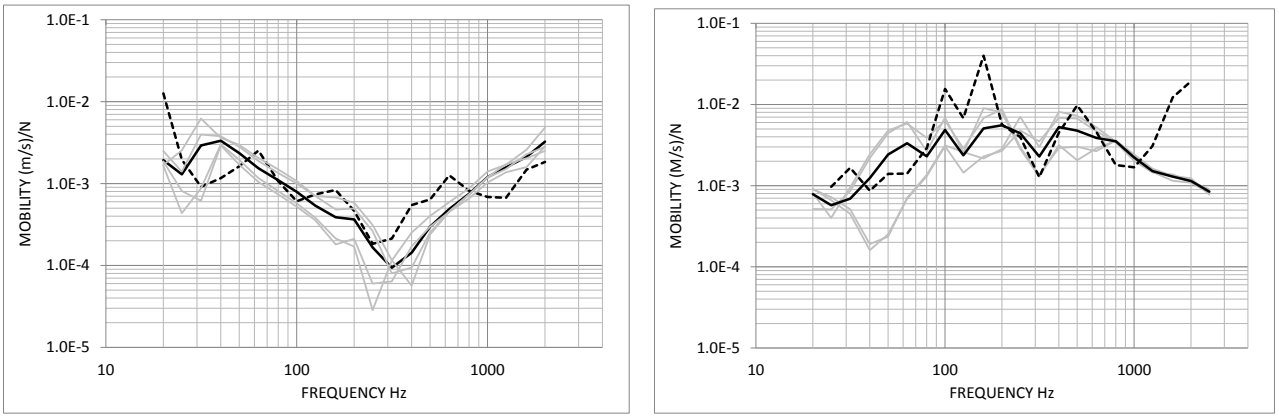

Figure 5. Left: pump mobility: measured magnitude of point mobility at four contacts (grey lines); average of measured values (black); RPM estimate (dashed); right: for fan.

Two fan points have a mobility within 3 dB of the 20mm plate mobility at 40 Hz and will contribute more to the total power into the low mobility reception plate than the other two fan point mobilities. Conversely, the other two fan points have mobilities within 3 dB of the perforated plate mobility at 63 Hz and will contribute more to the total power into the high mobility reception plate. The two stage RPM estimate of source mobility therefore is not able to track the average measured value. In general, the RPM works best with sources where the point mobilities at the contacts are similar.

3. Installed power by RPM

The RPM quantities were used to predict the powers from the pump and from the fan when attached to other plate structures: a framed notched plate of 11 mm aluminium of size 2.18m x 1.56m. Notches at the edges give a rotationally compliant thickness of 3mm. In addition, the pump then was attached to a 13mm ribbed Perspex plate, with dimensions 1m x 1m. The ribs are of dimension 50mm x 13mm, at 120mm centres. As a test of isolator efficiency, the pump was first rigidly attached to the two structures and then when mounted on rubber isolators. Again, and for comparison, the structure-borne powers of the sources, when attached to the plates, were measured using equation (2). For the RPM estimate of power, the receiver plate mobility was measured as the spatial average of the point mobility.

The measured and RPM estimated powers from the pump into the 11 mm plate are shown in Figure 6, left. The RPM estimate is within 10 dB of the measured power at frequencies above 40 Hz, with larger discrepancies below this frequency. For the fan power, shown in Figure 8, right, the tonal component at 50 Hz is predicted and elsewhere, prediction is within 10 dB of the measured power.

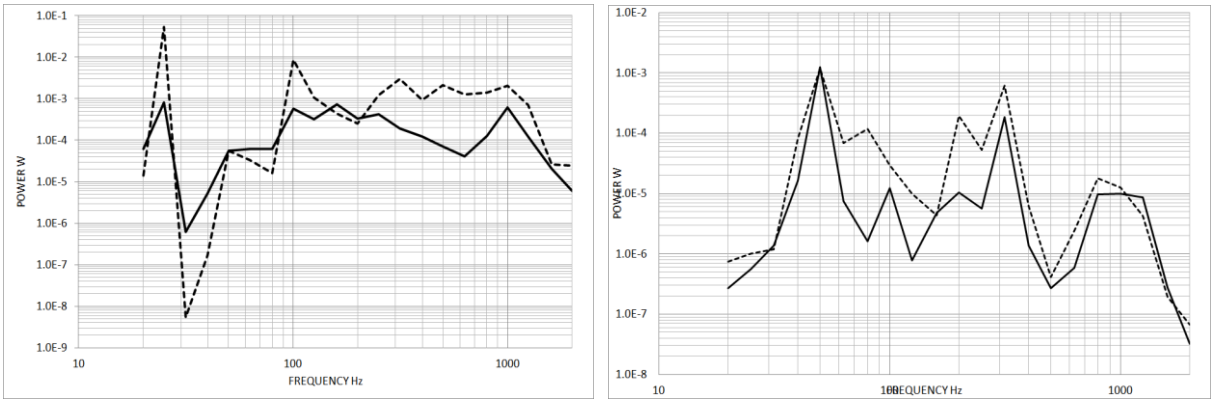

Figure 6. Left: measured pump power (solid line) and RPM estimate (dashed) into 11 mm plate; right: fan power.

Of interest is the use of the RPM in assessing the efficiency of isolators on a power basis, when in the installed condition. The calculated installed power requires only the blocked force squared, if it is assumed that the isolator mobility is greater than the source mobility and the receiver mobility. Referring to equation (5), the installed power

$$P_{installed} \approx F_{beq}^2 \, \mathrm{Re}\,(Y_{receiver}) \qquad (11)$$

In this case, F_{beq}^2 is the blocked force squared, obtained from mounting the isolated pump on the low mobility 20mm plate. Figure 7, left shows the measured and RPM estimated power from the isolated pump into the 11mm plate. The agreement is within 10 dB. The overestimates at frequencies above 100 Hz are due to low signal-noise.

The power insertion loss of the isolators is obtained from Figure 6, left, and Figure 7, left. Figure 7, right, shows that the isolators perform least well at 25 Hz, the first tonal frequency of the pump, but give significant isolation above 100 Hz.

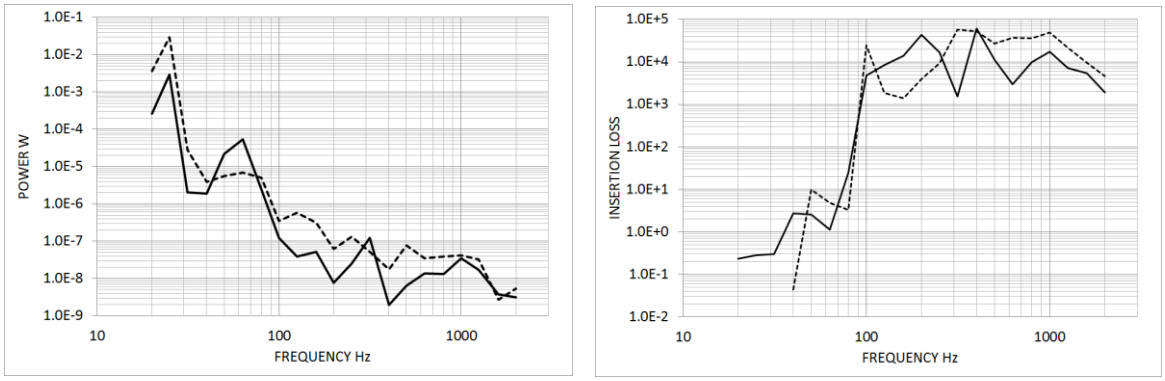

Figure7. Left: measured power (solid line) and RPM estimate (dashed) of isolated pump into 11 mm plate; right: measured (solid) and RPM estimate (dashed) of power insertion loss.

Figure 8 shows the pump on the perspex ribbed plate, left, when rigidly attached and right, when on isolators.

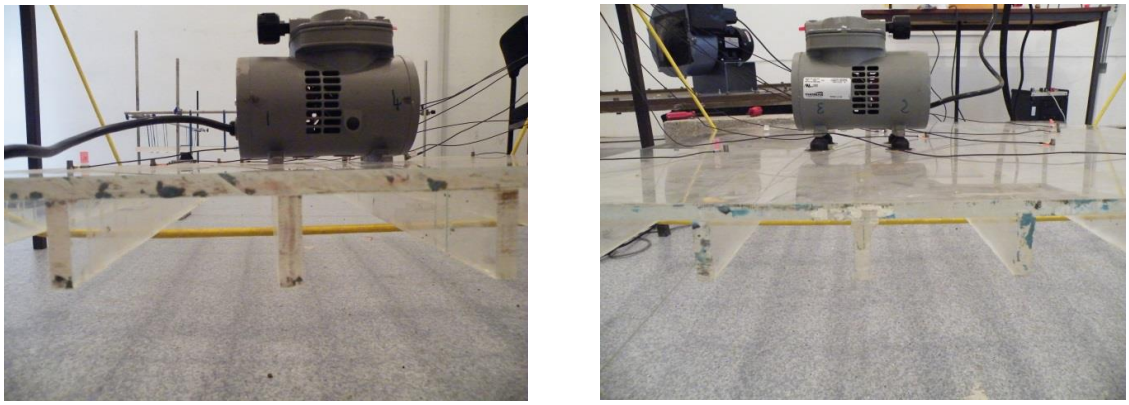

Figure 8. Ribbed Perspex plate with left: pump rigidly attached, and right: with pump on isolators.

Figure 9, left shows the measured and RPM estimated powers from the rigidly attached pump. The RPM captures the important tonal components and estimates are within 5 dB of the measured powers, up to 300 Hz, and within 10 dB above 300 Hz. Figure 9, right shows the power from the pump on isolators. The RPM estimates are within 5 dB of the measured powers, over most of the frequency range. Again, comparison of the powers gives the insertion loss of the isolators, which relates to the reduction in sound pressure in the far field.

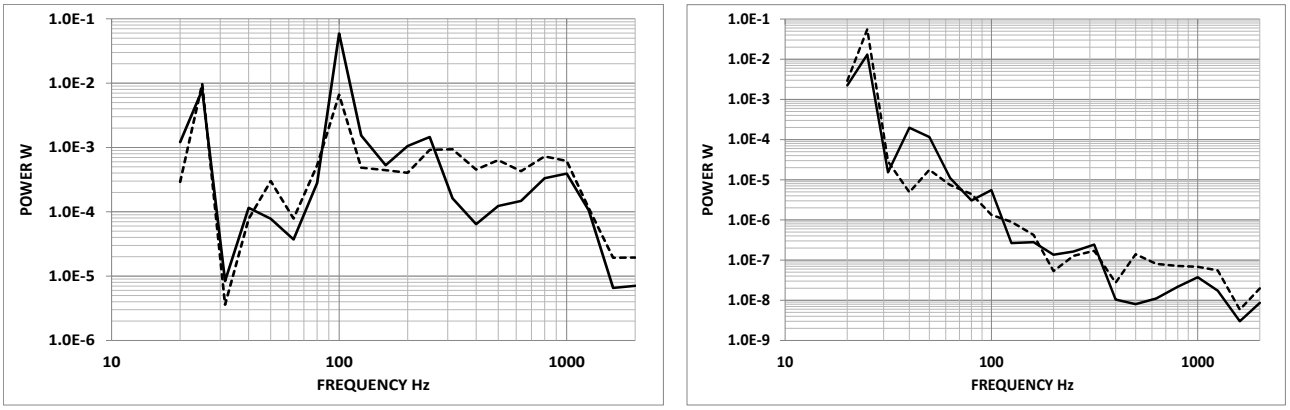

Figure 9. Pump power into ribbed plate: measured (solid line), by RPM (dashed); left: rigidly attached; right: on isolators.

4. Uncertainties in the two stage RPM

The data reductions, implicit in the two stage reception plate method, generate uncertainties at each step of the measurement procedure. In particular, phase information is lost in spatial and spectral averaging. The modal behaviour of the reception plates and of plate-like building elements, 'colour' the frequency spectra of the source quantities. As in other areas of building acoustics, spatial averaging (e.g. representing the mobilities at the contact points of a machine base as a single mobility) is appropriate when there are small spatial variations.

In an investigation of uncertainty, Putra and Mace use possibilistic and probabilistic approaches to multiple contact sources on infinite and finite plates [16]. Vogel et al [17] assess the error propagation in the two stage method by partially differentiating the power expression in equation (10) with respect to five quantities: power into the low mobility reception plate; real part of plate mobility; power into high mobility reception plate; real part of plate impedance; mobility of the receiving structure. Assigning uncertainties of 1 dB to each of the input values gives an uncertainty of 4.5 dB in the transmitted power. Assigning uncertainties of 2 dB to each of the input values gives an uncertainty of 7 dB in the transmitted power.

In this study, the uncertainty in the estimates of source quantities is assessed in terms of the sample standard deviations measured throughout the two stage RPM. The cases considered are those of the fan and of the air pump, without and with isolators. Figure 10 provides a schematic of the measurement process and the components of uncertainty. A log-normal distribution is assumed and results are presented in decibels ref 10^{-12} on a power basis, to provide similar terms before they are combined. It is recognised that a significant cause of uncertainty is the modal behaviour of the reception plates, particularly at low frequency, which will affect the spatial sampling in several of the steps. However, the sample sizes and source/accelerometer locations differed in the steps and it therefore is assumed that the contributing uncertainties were not correlated.

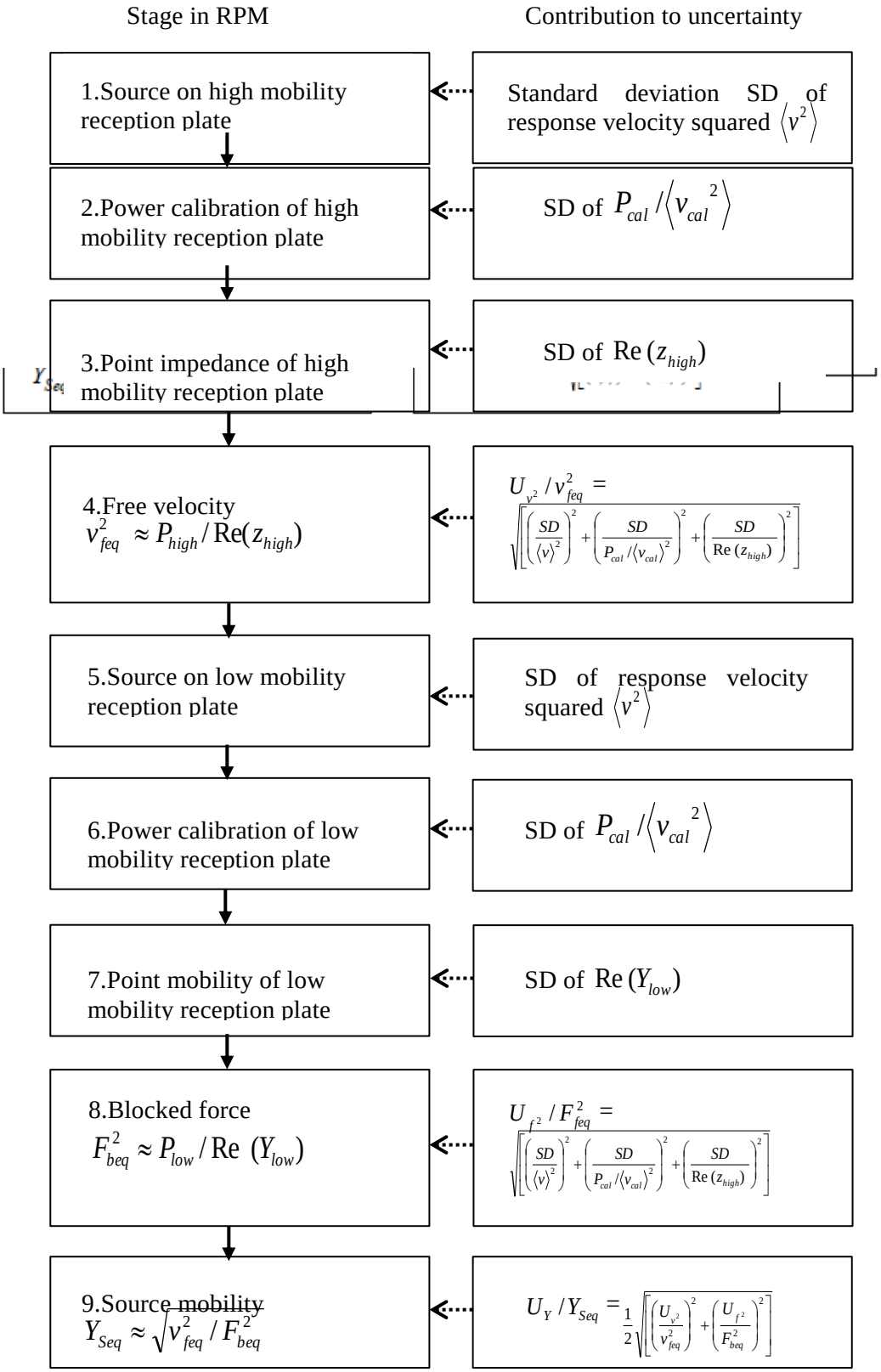

Figure 10. Schematic of steps in the two stage RPM and components of uncertainty.

4.1. Uncertainties for the pump

The first component of uncertainty (step 1 in Figure 10) is due to the variation in response velocity squared of the high mobility perforated plate when the attached pump is in operation. Figure 11 shows the mean and sample standard deviation from 4 accelerometer positions and 3 pump locations.

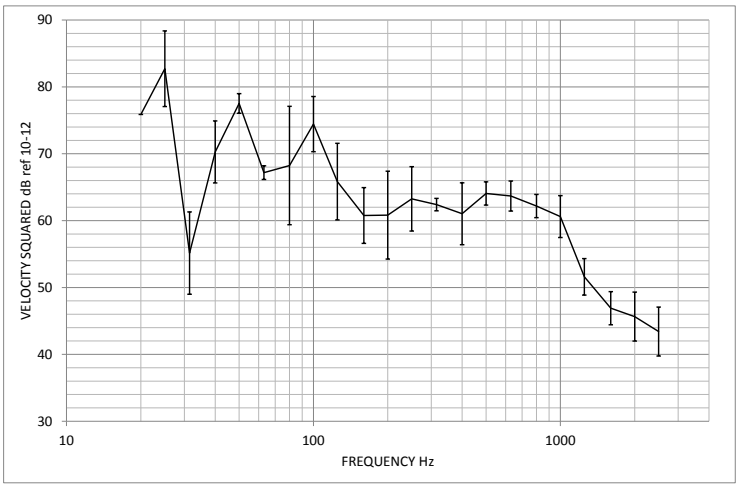

Figure 11. Perforated plate velocity squared with pump operating: mean and standard deviation.

The standard deviation is of the order of 5 dB at low frequencies, due to the modal behaviour of the reception plate. The standard deviation converges to 3 dB with frequency, with a larger value 4 dB at high frequencies due to reduced signal-to-noise.

The second component is in the power calibration of the high mobility reception plate (step 2). Figure 12 shows the average and sample standard deviation from 5 accelerometer positions and 12 shaker locations.

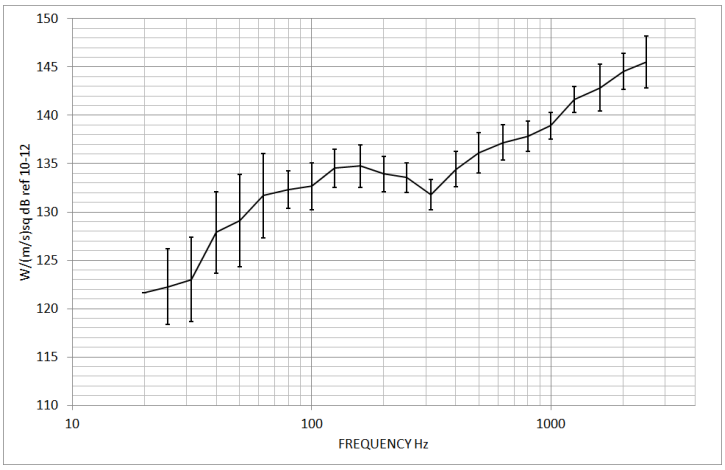

Figure 12. Power calibration of perforated plate: mean and standard deviation.

The standard deviation is of the order of 4 dB at low frequencies, again due to the modal behaviour of the reception plate, and converges to 2 dB at mid frequencies, with a larger value 3 dB at high frequencies due to reduced signal-to-noise.

Step 3 concerns the real part of the point impedance of the high mobility reception plate.

Figure 13 shows the mean and sample standard deviation from 12 shaker locations. The sample standard deviation converges with increased frequency from 6 dB to 3 dB.

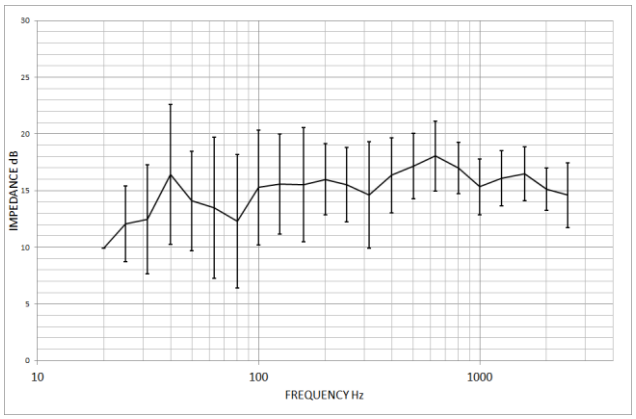

Figure 13. Mean and standard deviation of real part of impedance of perforated plate.

Combining the standard deviations as standard uncertainties (step 4) [18], gives the uncertainty in the estimate of the pump free velocity squared in Figure 14.

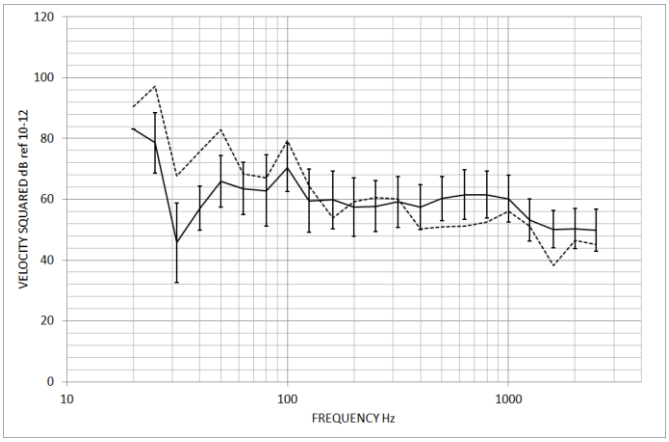

Figure 14. Pump sum squared free velocity: measured (dashed) and RPM estimate (solid line) with uncertainty.

The uncertainty in the RPM estimate varies from 14 dB at low frequency, converging to 6 dB at high frequency. The differences between the RPM estimates and measurement are within the uncertainty at frequencies above 50 Hz. The low frequency discrepancies of 10 dB highlight the limitation of this method for sources, which are rigid body and tonal.

The process is repeated for the operating pump rigidly attached to the low mobility reception plate of 20 mm aluminium (step 5). Figure 15 shows the average response velocity squared and sample standard deviation from 4 accelerometer positions and two pump locations.

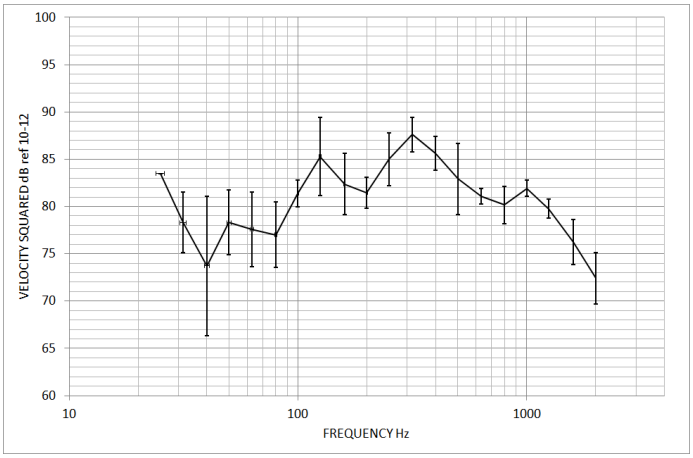

Figure 15. Response velocity squared of 20mm plate with pump operating: mean and standard deviation.

The standard deviation varies from 7 dB at low frequencies to 2 dB at mid frequencies, with an increase to 3 dB at high frequency due to reduced signal-to-noise.

The 20 mm plate has a lower modal density than the 1 mm perforated plate and greater spatial variations in values are expected. Surprisingly, this is not evident in the power calibration (step 6) in Figure 16, for 5 accelerometer positions and 5 shaker locations. The sample standard deviation is 3 dB or less, over the whole frequency range. This may be due to the effects of modal behaviour, on the calibration power and average square plate velocities, partially cancelling in the ratio $P_{cal}/\langle v_{cal}{}^2 \rangle$.

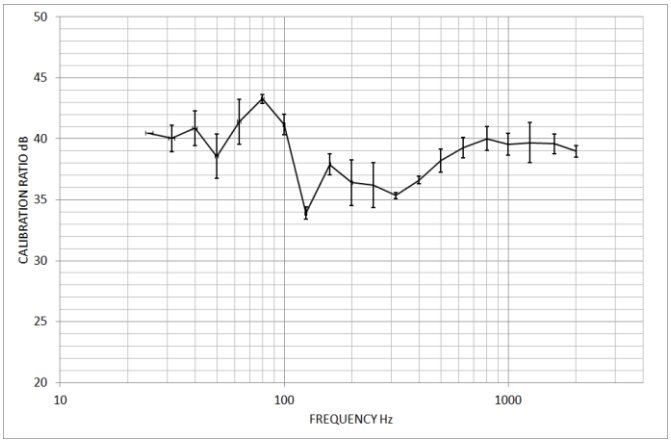

Figure 16. Power calibration of 20mm plate: mean and standard deviation.

Figure 17 shows the average real part of the point mobility of the low mobility reception plate from 16 shaker locations (step 7). The standard deviation is within 3 dB over the whole frequency range, with convergence to 1 dB at high frequency.

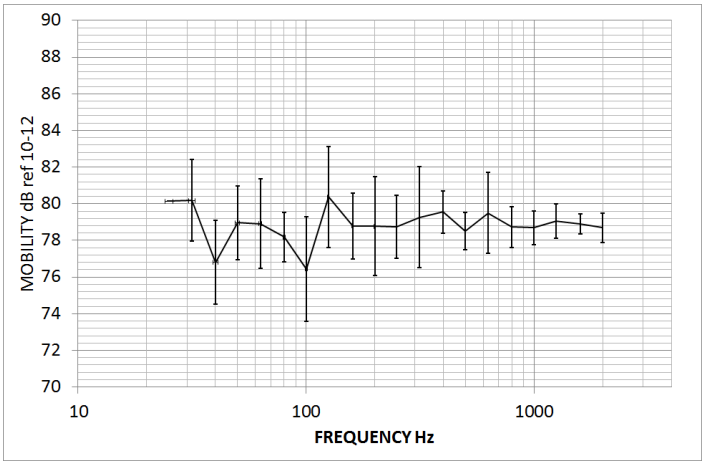

Figure 17. Real part of point mobility of 20mm plate: mean and standard deviation.

Combining the sample standard deviations as standard uncertainties (step 8) gives the uncertainty in the estimate of the pump blocked force squared in Figure 18. The uncertainty converges from 10 dB at low frequency to 5 dB at high frequency.

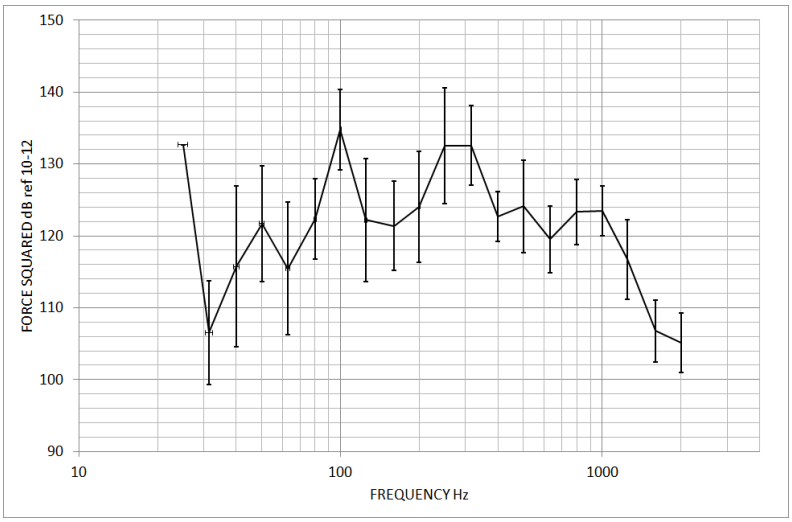

Figure 18. RPM estimate of pump sum squared blocked force with uncertainty.

It remains to combine the results of the eight steps to obtain the source mobility (step 9). Figure 19 shows the measured average point mobility magnitude, with RPM estimate and uncertainty. The uncertainty in the RPM estimate varies from 8 dB at low frequency to 6 dB at high frequency. The largest discrepancy between measured and RPM estimate is of the order of 5 dB and is within this limit.

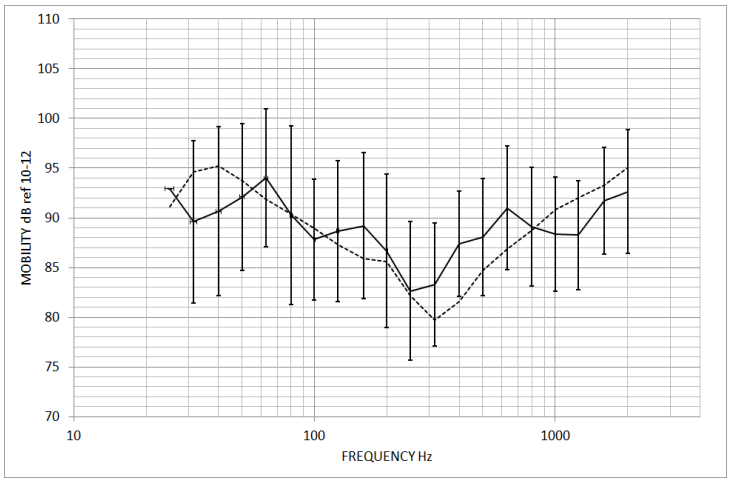

Figure 19. Pump mobility: measured magnitude (dashed) and RPM estimate (solid line) with uncertainty.

For completeness, Figure 20 shows the RPM estimate of blocked force squared of the isolated pump. This source quantity only is required for predicting the installed power if equation (5) can be assumed to apply for all receiver structures. The uncertainty is of the order of 5 dB over the frequency range.

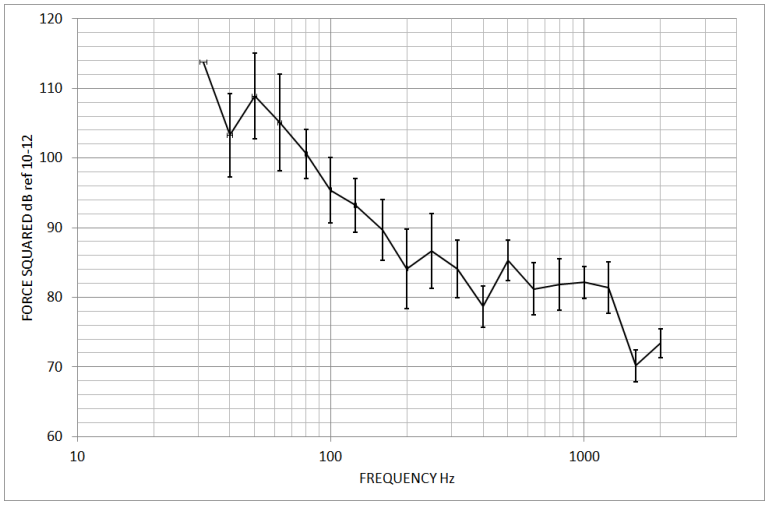

Figure 20. RPM estimate of sum squared blocked force of isolated pump, with uncertainty.

4.2. Uncertainties for the fan

The process was repeated for the fan and results are presented for steps 1, 4, 5, 8 and 9 of Figure 10. The other steps: 2, 3, 6, 7 i.e. the power calibrations and mobility/impedance of the reception plates, were the same as for the pump and are not shown. Figure 21 shows the standard deviations, and the uncertainties based on them, for steps 1, 4, 5 and 8. The response velocity squared of perforated plate (upper left) was from 8 accelerometer positions and 2 fan locations. The response velocity squared of the 20 mm plate (lower left) was from 4 accelerometer positions and one fan location. The uncertainty in the RPM estimate of the sum square free velocity (upper right) varies from 12 dB at low frequency to 6 dB at high frequency. The uncertainty in the RPM estimate of the sum square blocked force (lower right) varies from 8 dB at low frequency to 2 dB at high frequency.

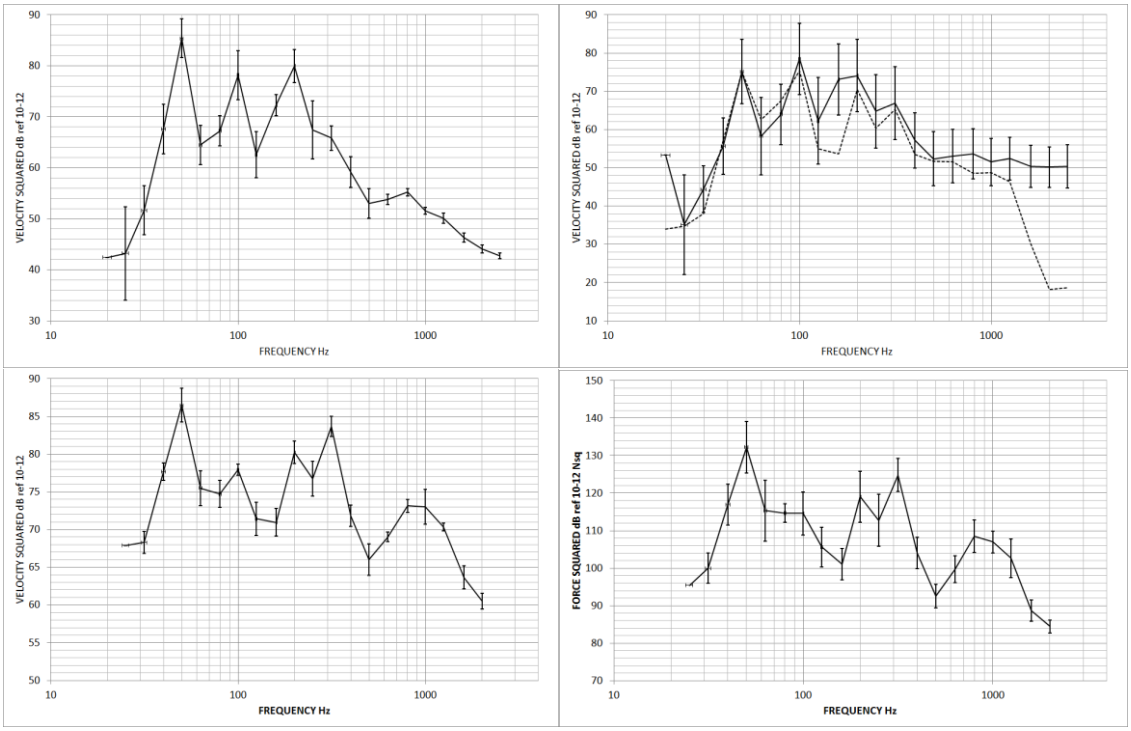

Figure 21. Fan on reception plates: upper left: perforated plate squared velocity with standard deviation; upper right: measured sum squared free velocity (dashed) and RPM estimate (solid line) with uncertainty; lower left: average velocity squared of 20 mm plate with standard deviation; lower right: RPM estimate of sum squared blocked force, with uncertainty.

Again, it remains to combine the results of the eight steps to obtain the fan mobility (step 9). Figure 22 shows the measured average point mobility magnitude, with RPM estimate and uncertainty. The uncertainty in the RPM estimate varies from 8 dB at low frequency to 6 dB at high frequency. The largest discrepancy between measured and RPM estimate is 8 dB at 160 Hz, but elsewhere the discrepancy is within the uncertainty for frequencies up to 1600 Hz. Also shown is the two stage estimate from combining the directly measured sum square free velocity and the RPM estimate of blocked force. The agreement is within 3 dB of the measured average point mobility, over the whole frequency range except at 800 Hz.

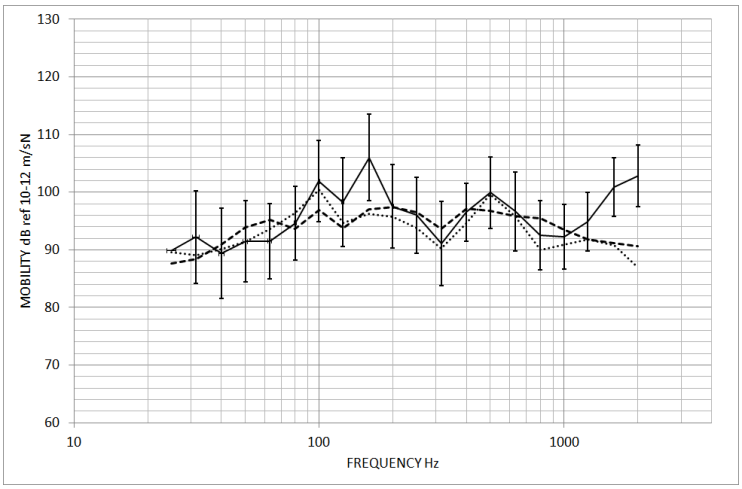

Figure 22. Fan mobility: RPM estimate (solid line) with uncertainty, measured (dashed), RPM estimate with measured free velocity squared (dotted).

5. Concluding remarks

The proposed method of characterizing structure-borne sources has identified the sum square free velocity and sum square blocked force as candidate independent quantities for sources connected through multiple contacts to plate-like receiver structures. Also required is the source mobility, which is obtained indirectly from the square root of the ratio of sum square free velocity and sum square blocked force.

The sum square free velocity and sum square blocked force can be measured by the two-stage reception plate method (RPM), i.e. by measuring the source power when attached to a high mobility plate and then a low mobility plate, respectively. The measurements and calculations are in one-third octave bands.

The uncertainty in the estimates of source quantities was explored in case studies of two sources: a compact pump and a medium size fan. The uncertainties were estimated from the sample standard deviations at each stage of the two stage RPM.

For the compact pump, the uncertainty in the RPM estimate of free velocity squared ranged from 14 dB at low frequency to 6 dB at high frequency. The RPM under-estimates of free velocity and blocked force at low frequencies are due to rigid-body rocking motion, which gives reduced power into the reception plates. However, the under-estimates partially cancel, for the estimates of source mobility and then for the calculated installed power into other plate-like structures. For the source mobility the uncertainty in the RPM estimate ranged from 8 dB at low frequency to 6 dB at high frequency.

For the fan, the uncertainty in the RPM estimate of free velocity squared ranged from 12 dB at low frequency to 6 dB at high frequency. For the source mobility the uncertainty in the RPM estimate ranged from 8 dB at low frequency to 6 dB at high frequency.

The two stage RPM involves spatial averaging and, as in other areas of acoustics, this works best when there are small spatial variations. This is exemplified in the RPM estimate of source mobility of the compact pump.

This investigation was limited to two sources and the sample sizes, at each stage of the RPM, were limited by the availability of transducers and signal channels. The conclusions therefore are not general. It is likely that a more rigorous sampling strategy will reduce the uncertainty in the estimates of the source quantities. However, the loss of phase information, as a result of spatial and spectral averaging, is still likely to yield large uncertainties at low frequencies and for tonal sources.

Acknowledgement

The authors wish to thank colleagues at Boeing Commercial Airplanes, at ITT Enedine Inc. and at LORD Corporation, for their helpful comments and financial support during this collaborative programme. Andrew Moorhouse and Andrew Elliott, of Salford University, provided important information from their parallel work on precise methods. Michel Villot, Convener of the European Working Group CEN/TC 126/WG07, and Carl Hopkins of Liverpool University are also thanked for sharing experiences of the related area of structure-borne sound transmission in lightweight buildings.

References

1. L. Cremer, M. Heckl and B.A.T. Petersson, Structure-borne Sound, 3rd ed., 607 p., Springer Berlin Heidelberg New York (2005).
2. B.A.T. Petersson and B.M. Gibbs, Towards a structure-borne sound source characterization, Appl. Acoustics 61, 325-343 (2000).
3. J.M. Mondot and B.A.T. Petersson, Characterisation of structure-borne sound sources: The source descriptor and the coupling function, J. Sound Vib. 114(3), 507-518 (1987).
4. C. Hoeller and B. M. Gibbs, Indirect determination of the mobility of structure-borne sound sources, J. Sound Vib. 344, 38-58 (2015).
5. S. H. Yap and B. M. Gibbs, Structure-borne sound transmission from machines in buildings, part 2: Indirect measurement of force and moment at the machine-receiver interface of a single point connected system by a reciprocal method. J. Sound Vib. 222 (1), 99-113 (1999).

6. A R Mayr and B M Gibbs, Single equivalent approximation for multiple contact structure-borne sound sources in buildings, Acta Acustica united with Acustica 98, 402-410 (2012).
7. J. Scheck and B. M. Gibbs, Impacted lightweight stairs as structure-borne sound sources, Applied Acoustics 90, 9-20 (2015).
8. M.M. Spaeh and B.M. Gibbs, Reception plate method for characterization of structure-borne sources in buildings: Assumptions and application, Appl. Acoustics 70, 361-368 (2009).
9. C. Hopkins and M. Robinson, Using transient and steady-state SEA to assess potential errors in the measurement of structure-borne sound power input from machinery on coupled reception plates, Applied Acoustics 79, 35-41 (2014).
10. M. Ohlrich, L. Friis, S. Aatola, A. Lehtovaara, M. Martikainen, O. Nuutila, Round Robin test of technique for characterizing the structure-borne sound-source-strength of vibrating machines, Euronoise (2006).
11. A.T. Moorhouse, On the characteristic power of structure-borne sound sources, J. Sound Vib. 248(3), 441-459 (2001).
12. B.M. Gibbs, N. Qi and A.T. Moorhouse, A practical characterization for vibro-acoustic sources in buildings, Acta Acustica united with Acustica 93, 84-93 (2007).
13. B.M. Gibbs, R. Cookson and N. Qi, Vibration activity and mobility of structure-borne sources by a reception plate method, J. Acoust. Soc. Am. 123(6), 4199-4209 (2008).
14. B. M. Gibbs, Uncertainties in predicting structure-borne sound power input into buildings, J. Acoust. Soc. Am. 133(5), 2678-2689 (2013).
15. B.A.T. Petersson and J. Plunt, On effective mobilities in the prediction of structure-borne sound transmission between a source structure and a receiver structure, part 1: Theoretical background and basic experimental studies, J. Sound Vib. 82, 517-529 (1982).
16. A. Putra and B. R. Mace, The effect of uncertainty in the excitation on the vibration input power to a structure, Advances in Acoustics and Vibration, Volume 2013, Article ID 478389 (2013).
17. A. Vogel, O. Kornadt, V. Wittstock and W. Scholl, Assessment of the uncertainties using the "two-stage method" for the characterization of structure-borne sound sources, Proc. Inter-noise 2015, San Francisco (2015).
18. H. Castrup, Estimating and combining uncertainties, Proc. 8th Annual ITEA Instrumentation Workshop, Lancaster Ca. (2004).